https://doi.org/10.5194/egusphere-2025-2304
Preprint. Discussion started: 17 June 2025

How can building representation influence flood hazard and impact modelling: Insights from the 2021 Ahr Valley Flood

Shahin Khosh Bin Ghomash[1], Nithila Devi Nallasamy[1], and Heiko Apel[1]
[1]Section Hydrology, GFZ German Research Centre for Geosciences, Potsdam (Germany)
Correspondence: Shahin Khosh Bin Ghomash (shahin@gfz.de)

Abstract. The increasing flood risk in urban areas, driven by rising urbanization and climate change, underscores the need for accurate representation of buildings and urban features in flood hydrodynamic models. This study investigates the impact of different building representation techniques on flood hydrodynamic and impact modeling, using the 2021 flood event in the Ahr Valley, Germany, as example. Three methods — Building Block (BB), Building Hole (BH), and Building Resistance (BR) —are applied across varying model resolutions to assess their influence on flood extent, water depths, and flow velocities.

Our findings reveal that building representation affects both simulated flood extent and flow dynamics. The Building Block and Building Hole approaches generally lead to larger flooded areas with deeper water and higher velocities, while increased resistance or omitting buildings results in smaller flood extents, shallower water, and slower flow. Additionally, we show a strong link between building representation and model resolution. Our findings show that at coarser resolutions, the choice of building representation is more critical, with larger differences in flood extent across setups. We show that while all methods produce acceptable flood extents, variations in water depths and velocities highlight the importance of choosing the right building representation for accurate flood simulations—particularly in dense urban areas where accurate flood impact assessments rely on realistic flow dynamics. Our results emphasize the importance of selecting appropriate building representation methods based on model resolution to enhance urban flood modeling and impact assessment accuracy, with a general recommendation to include buildings as physical obstacles (BH, BB) in hydraulic models.

1 Introduction

The changing climate is causing an increase in both the frequency and intensity of extreme weather events, resulting in more frequent and severe floods (Skougaard Kaspersen et al., 2017). Hydrodynamic models are becoming increasingly important for assessing the impact of floods and are widely used in flood management planning and risk assessments (Merz et al., 2020). However, due to the limited availability of high-resolution data and the complexity of urban landscapes, accurately modeling and forecasting urban floods remains a significant challenge for researchers and policymakers.

Uncertainties in hydrodynamic modeling can stem from various sources, such as the model structure, parameters, and boundary conditions. These factors can significantly influence the reliability and accuracy of the model's performance (Caviedes-Voullième et al., 2020; Alipour et al., 2022). Among the various sources of uncertainty related to model structure and parameters, topographic data have been recognized as one of the key factors influencing the accuracy of flood simulations (Sharma and

https://doi.org/10.5194/egusphere-2025-2304
Preprint. Discussion started: 17 June 2025

Regonda, 2021; Jiang et al., 2022). Catchment topographic features are known to play a significant role in controlling the spatial distribution of runoff dynamics and influencing surface runoff connectivity (Khosh Bin Ghomash et al., 2019; Nithila Devi and Kuiry, 2024). Typically in urban areas, a significant portion of the surface topography is made up of buildings. Previous research has shown that buildings can significantly impact flood volume and flow propagation through a combination of storage, obstruction, and resistance effects (Bruwier et al., 2018; Shen and Tan, 2020). Buildings walls may obstruct the flow or the flow may pass through building structures at reduced speeds if the main entrance or windows are open, or if the floodwater rises above the height of the entrance threshold. (Wang et al., 2010).

In urban flood modeling, various building treatment methods have been proposed to address these effects, including the buildings block, building resistance and building hole approaches (Schubert and Sanders, 2012; Jiang et al., 2022; Iliadis et al., 2024). In the buildings block method, the elevation of building footprints is raised to to a certain height or in case of availability of detailed building data, to the rooftop level of each building. An example of this can be found at Hunter et al. (2008), where building footprints in an urban catchment area in the UK were elevated by 12 meters for larger houses and 6 meters for smaller houses. The building resistance method, as also discussed by Alcrudo (2004); Néelz and Pender (2007), increases the surface friction coefficient in areas where buildings are located. In the building hole approach, building footprints are excluded from the computational grid, functioning as reflective boundaries, which is equivalent to the building block method with infinite building heights. This method has been widely used in previous studies, e.g. Apel et al. (2022, 2024); Khosh Bin Ghomash et al. (2022, 2023, 2025a). Although in recent years the concept of Urban Porosity has been introduced to parameterize building effects with an emphasize on computational efficiency (Dewals et al., 2021), it is still not widely adopted in flood modeling applications. Further on, this method often fails to capture fine-scale flow dynamics, such as localized wave reflections and flow channeling around individual buildings, leading to reduced accuracy in high-resolution simulations (Kim et al., 2015), critical for detailed flood risk assessments.

The 2021 flooding event in the Ahr Valley, Germany, serves as a stark reminder of the devastating impact extreme weather events can have. In July 2021, the region was hit by a catastrophic flood, leading to loss of life, displacement of residents, and widespread damage to infrastructure, homes, and landscapes (Mohr et al., 2022). Of the 184 fatalities recorded in Germany, 133 occurred along the Ahr River, a tributary of the Rhine. Although relatively small in size (approximately 900 km^2), the Ahr River basin features morphological characteristics—such as narrow channels confined within gorges—that limit its capacity to accommodate sudden water surges. This challenging topography becomes even more complex in urbanized areas like Bad Neuenahr-Ahrweiler, a densely built town with a population of around 26,500 (Truedinger et al., 2023), which was severely affected by the July 2021 flood. Such conditions naturally raise the question of how to adequately represent urban structures within complex terrain to ensure reliable flood hydrodynamic simulations.

This study investigates how different building representation methods influence hydrodynamic modeling and flood impact analysis for the July 2021 flood event. We apply three commonly used approaches—building block, building resistance, and building hole—to evaluate their effects on predicted flood extent and flow characteristics, and also include a baseline scenario where buildings are not explicitly represented in the domain. Moreover, since model resolution plays a key role in both the feasibility and accuracy of urban flood simulations—and is often limited by computational resources or the availability of

https://doi.org/10.5194/egusphere-2025-2304
Preprint. Discussion started: 17 June 2025

high-resolution data—we examine how these building representation methods interact with different grid resolutions by testing spatial resolutions ranging from 1m to 10m. Finally, we assess whether the differences in hydraulic behavior caused by these modeling choices have a significant impact on flood impact assessment outcomes.

2 Case Study

The Ahr River, an 86 km-long tributary of the Rhine, flows through the federal states of Rhineland-Palatinate and North Rhine-Westphalia in Germany. Our study area (Figure 1) focuses on the downstream section of the river, spanning roughly 30 km from the towns of Altenahr to Sinzig. In this stretch, the valley is narrow and enclosed in the upper third, gradually widening as it extends downstream toward the Rhine.

This region is characterized by a complex urban-rural landscape, with a mix of small settlements and the relatively larger urban area of Bad Neuenahr-Ahrweiler, which has a population of around 26,500 (Truedinger et al., 2023). The valley's urban development is particularly dense in certain areas, where infrastructure, residential buildings, and commercial establishments are concentrated in flood-prone zones. This urban sprawl has significantly altered the natural flow of the river and increased the vulnerability of built structures. The surrounding rural areas, while less densely populated, also feature extensive agricultural land use, contributing to the overall complexity of the landscape. Despite the region's rural nature, the urban complexity and building infrastructure play a critical role in how floodwaters interact with the environment. The area's average annual precipitation is around 675 mm, which is below the German national average (Truedinger et al., 2023).

In mid-July 2021, the Ahr Valley experienced one of the most catastrophic flood events in recent history, as heavy rainfall triggered rapid flooding across much of Western and Central Europe, severely affecting Belgium, the Netherlands, and Germany (Schäfer et al., 2021). The Ahr Valley was among the hardest-hit regions, accounting for around 70 percent of all flood-related fatalities in Germany (Truedinger et al., 2023). The flood's impact was exacerbated by a combination of steep slopes, narrow valleys, and the dense concentration of buildings in vulnerable zones. Over centuries, the valley has been extensively settled and cultivated, with urban infrastructure often built in areas prone to rapid flow concentration, mass movement, and debris accumulation. The narrowness of the valley, combined with the built environment, contributed to the rapid intensification of floodwaters. During the flood on July 14, 2021, water levels in the Ahr River reached their highest on record at the gauging stations, with depths peaking around 10 meters at Altenahr station (Mohr et al., 2022). However, due to widespread damage and destruction of the gauging stations during the event, precise water levels remain uncertain (Schäfer et al., 2021).

https://doi.org/10.5194/egusphere-2025-2304
Preprint. Discussion started: 17 June 2025

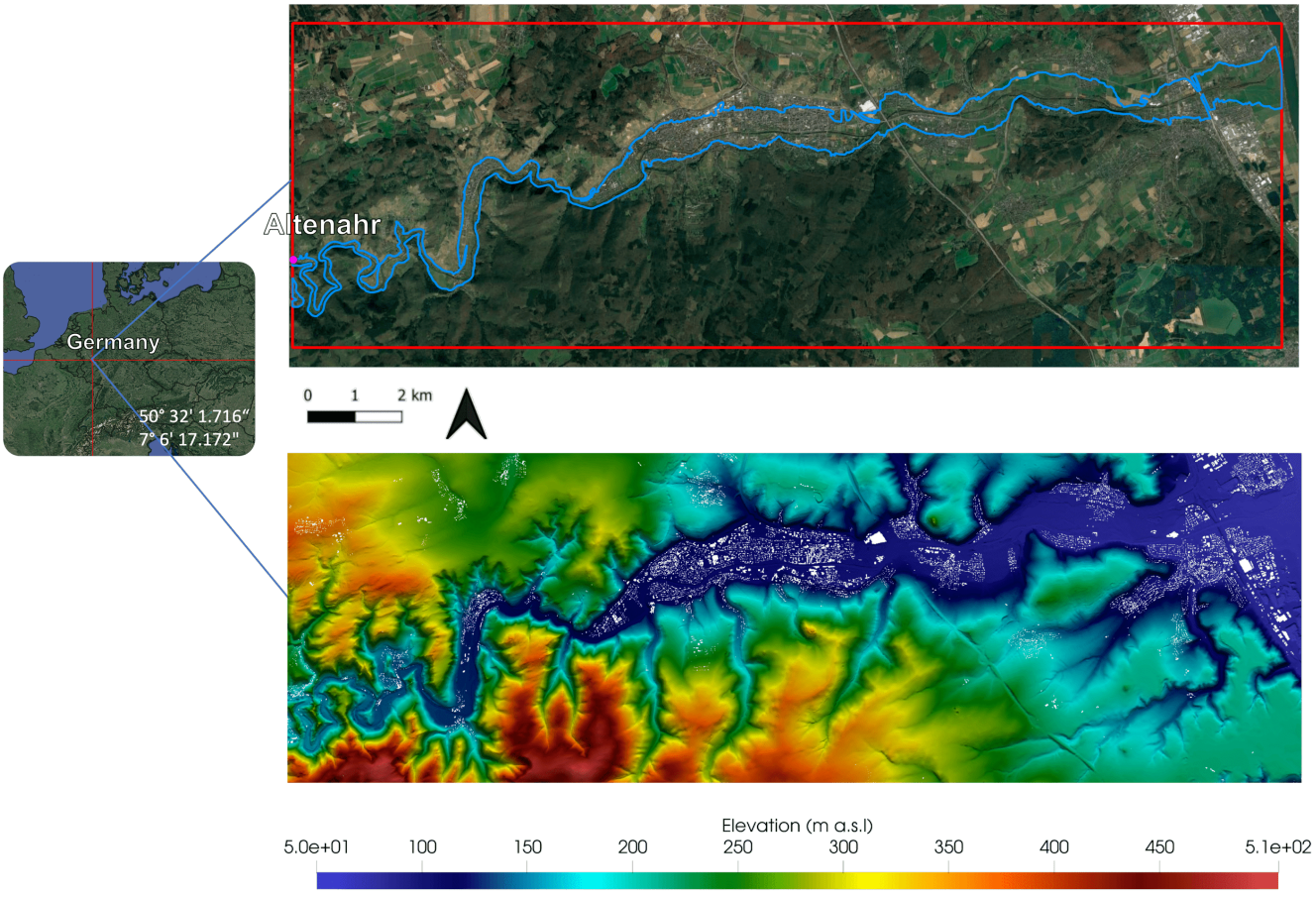

Figure 1. The red line in the upper panel marks the boundary of the simulation domain, while the lower panel displays the topography. In the upper panel, the purple point indicates the location of the Altenahr gauge station. The blue line shows the maximum flood extent observed during the 2021 flood event. Satellite imagery © Google Earth 2025.

3 Methods

3.1 Hydrodynamic model: RIM2D

RIM2D is a two-dimensional, raster-based hydrodynamic model developed by the Section Hydrology at the German Research
90 Centre for Geosciences (GFZ) in Potsdam, Germany. It is designed to solve the local inertia approximation of the Shallow Water equations, as outlined by Bates et al. (2010), which has proven effective for flood inundation modeling (Falter et al., 2014; Neal et al., 2011; Apel et al., 2022, 2024; Khosh Bin Ghomash et al., 2024, 2025a). The model operates on a structured grid of square raster cells, which provides a computationally efficient framework for representing terrain and flow dynamics across large domains while maintaining spatial consistency.

https://doi.org/10.5194/egusphere-2025-2304
Preprint. Discussion started: 17 June 2025

The local inertia formulation provides a more accurate representation of water flow dynamics compared to simpler models, such as the diffusive wave model (De Almeida and Bates, 2013; Caviedes-Voullième et al., 2020), by introducing a term that accounts for the rate of change in local fluid momentum. This term influences how momentum is transferred from one time step to the next, meaning that the flow at any given time step affects the subsequent step by requiring acceleration from its previous state. As the local inertia approximation neglects the convective acceleration terms and as a consequence decouples the fluxes in x and y directions. Thus, the fluxes F and G are reduced to:

$$\mathbf{F} = \begin{bmatrix} q_x \\ \frac{1}{2}gh^2 \\ 0 \end{bmatrix}, \quad \mathbf{G} = \begin{bmatrix} 0 \\ q_y \\ \frac{1}{2}gh^2 \end{bmatrix}. \tag{1}$$

In the shallow-water equations below:

$$\frac{\partial \mathbf{U}}{\partial t} + \frac{\partial \mathbf{F}}{\partial x} + \frac{\partial \mathbf{G}}{\partial y} = \mathbf{S}_b + \mathbf{S}_f, \tag{2}$$

Where:

$$\mathbf{U} = \begin{bmatrix} h \\ q_x \\ q_y \end{bmatrix}, \quad \mathbf{S}_b = \begin{bmatrix} 0 \\ -gh\frac{\partial z}{\partial x} \\ -gh\frac{\partial z}{\partial y} \end{bmatrix}, \quad \mathbf{S}_f = \begin{bmatrix} 0 \\ -\sigma_x \\ -\sigma_y \end{bmatrix}. \tag{3}$$

Where the conserved variables $\mathbf{U}$ are water depth h [L] and momentum components [L^2/T] in the Cartesian directions q_x and q_y. The vectors $\mathbf{F}$ and $\mathbf{G}$ represent the fluxes. The term $\mathbf{S}_b$ is the bed source term, where z is bed elevation [L]. The term $\mathbf{S}_f$ is the friction source term, where σ_x and σ_y are the friction slopes, here computed using Manning's equation. Finally, g is gravitational acceleration [L/T^2]. This formulation captures inertial effects more effectively than diffusive wave models, serving as a bridge between those simpler approximations and the more comprehensive full-dynamic equations.

While the original explicit numerical solution proposed by Bates et al. (2010) may become unstable under near-critical to super-critical flow conditions or with small grid cell sizes (De Almeida and Bates, 2013), RIM2D addresses these issues by incorporating the numerical diffusion method introduced by de Almeida et al. (2012). This enhancement stabilizes the solution across a wider range of flow regimes and grid resolutions. RIM2D is written in Fortran and has been coded for massive parallelization on Graphical Processor Units (GPU) through NVIDIA CUDA Fortran libraries. The model supports computations on multiple GPUs, enabling fast computation of high-resolution or large-scale models with a large number of computational raster cells and is available as open-source under the European Union Public License 1.2.

3.2 Data and model set-up

3.2.1 Spatial data and Building representation

In this study, we utilize the DGM1 digital elevation model (DEM) provided by the German Federal Agency for Cartography and Geodesy (BKG) for model setup. This DEM, with a resolution of dx = 1 meter, is generated through lidar mapping of the

https://doi.org/10.5194/egusphere-2025-2304
Preprint. Discussion started: 17 June 2025

area. To examine the interaction between building representation in the model and DEM resolution, the 1-meter DEM is also resampled by averaging into resolutions of 2, 5, and 10 meters, resulting in a total of four setups with different resolutions.

The 3D building model LoD1 Deutschland (LoD1-DE), produced by the German Federal Agency for Cartography and Geodesy (BKG), was used for buildings representation. In the LoD1 model, all buildings are represented as basic blocks, with their floor plans typically sourced from the official real estate maps. The dataset also provides the height of each individual building.

We implement seven different building representation scenarios for this study: no building (NoB), building blocks (BB), building hole (BH), and increased building resistance by factors of 2x (BR2x), 3x (BR3x), 5x (BR5x), and 10x (BR10x). These scenarios, combined with four different resolutions, result in a total of 28 setups. In the NoB scenario, no buildings are included in the domain, and no modifications are made to the DEM. In the building blocks (BB) scenario, the elevation of cells containing building footprints as in LoD1-DE is raised by the height of each building, also taken from the LoD1-DE building dataset. For buildings with missing height data, a default height of 6 meters is used, following Hunter et al. (2008). In the BH scenario, cells containing building footprints as in LoD1-DE are removed from the computational grid, functioning as closed reflective boundaries. In the increased resistance scenarios, the Manning roughness values of the cells containing building footprints are multiplied by 2, 3, 5, and 10 for the BR2x, BR3x, BR5x, and BR10x setups, respectively.

Manning roughness values for the domain were assigned according to the 2020 land cover classification of Germany, which was derived from Sentinel-2 data (Riembauer et al., 2021). The land cover classification is based on atmospherically corrected Sentinel-2 satellite imagery, processed using the MAJA algorithm and provided by the EOC Geoservice of the German Aerospace Centre (DLR). The classification utilizes training data derived from reference sources such as OpenStreetMap, as well as the Sentinel-2 imagery itself. This land cover dataset was selected for the study due to its relatively high spatial resolution of 10 meters. Additionally, the main channel of the Ahr River was manually incorporated as a separate land cover class. Appropriate Manning values were assigned to each land categories which are presented in Table 1 which also presents their respective percentage coverage in the simulation domain. It should be pointed out that while calibrating the model for each building scenario at every resolution could improve the accuracy of the results, the primary objective of this study is not calibration. Instead, the goal is to compare different scenarios under identical conditions and model settings in order to isolate the impact of varying building representations on simulation outputs. This approach is justified for several reasons. First, using consistent Manning values across scenarios to study building representation effects is a standard practice, as seen in studies like Schubert and Sanders (2012), Jiang et al. (2022), and Iliadis et al. (2024). Secondly, it is often unrealistic to expect detailed calibration data for every valley where a hydrodynamic model is deployed. In many cases, especially in operational contexts or data-scarce regions, the only feasible option is to use available spatial datasets and standardized parameterizations. While calibration is preferable, the lack of data (e.g., flood mapping) and the need for rapid model setup in operational contexts make uncalibrated models more realistic. For this reason, we deliberately avoid detailed calibration in this study, focusing instead on evaluating how changes in building representation, under standardized parameters and consistent and controlled model settings, influence the simulation results. The core objective is to compare the scenarios against one another to isolate the effects of different building representations, independent of calibration influences. While a comparison to observed flood data is also

https://doi.org/10.5194/egusphere-2025-2304
Preprint. Discussion started: 17 June 2025

included for context at the end of the manuscript, the primary focus remains on the internal consistency and relative differences between scenarios.

Land category	Manning roughness coefficient [$m^{-1/3}$ s]	Coverage [%]
Forest	0.084	52.17
Vegetation	0.055	18.82
Built-up/sealed areas	0.020	11.37
Bare soil	0.035	4.82
Agriculture	0.029	11.86
River channel	0.016	0.44
Waterbodies	0.050	0.52

Table 1. Land cover types, their corresponding Manning roughness coefficients, and their proportional coverage within the domain.

3.2.2 Flood event data for the inflow boundary

Inflow to the models is based on the reconstructed water levels (in meters above sea level) at the Altenahr gauge, provided by the flood warning center of Rhineland-Palatinate (Mohr et al., 2022). This reconstruction was necessary because the gauge was destroyed during the 2021 event. For model setup, the reconstructed water levels are applied to cells of the river cross section at the western boundary of the model domain. To account for overbank flow, additional cells adjacent to the river channel with elevations below the peak water level of the flood hydrograph were also included. Water depths are assigned to these cells only when river water levels surpass their elevations. The reconstructed water level timeseries at the Altenahr gauge, used as boundary condition in the model is depicted in Figure A1.

4 Results and discussion

4.1 Flood dynamics

Figure 2 presents the maximum inundated areas with water depths exceeding 1 cm and 100 cm for the following building scenarios: no building (NoB), building blocks (BB), building hole (BH), and increased building resistance by 2x (BR2x), 3x (BR3x), 5x (BR5x), and 10x (BR10x), across model resolutions of dx = 1, 2, 5, and 10 m. To allow for a clearer comparison, inundated cells corresponding to building footprints are excluded. Additionally, to highlight differences more clearly, the flooded area for each resolution is normalized by the flooded area of the NoB scenario and presented in subfigures b and d. The results show that the different building scenarios produce flood extents with variations of up to 15% for water depths exceeding 1 cm and up to 18% for depths above 100 cm. This indicates that building representation has a slightly greater impact on simulating deeper flooding, which typically causes the most significant damage during flood events. It is also worth noting that the BR10X scenario with the most increased surface resistance shows the greatest deviation in flooded areas compared

https://doi.org/10.5194/egusphere-2025-2304
Preprint. Discussion started: 17 June 2025

to other configurations. In contrast, differences in simulated flood extents among the other setups remain below 10% across all resolutions, indicating that building representation has a limited impact on overall flood extent. Moreover, the BB and BH setups show the highest flooded areas while the increased resistance setups result in the least flooded area, with the BR10X resulting in the smallest extents. Regarding the influence of model resolution, the most pronounced differences in flood extent among building scenarios are observed in the coarsest resolution (dx = 10 m), underscoring the critical role of building representation when dealing with coarser-resolution models. One reason for this can be due to the building cells being larger and occupying a greater portion of the domain in coarser setups, thereby exerting a stronger influence on flow dynamics during simulations.

https://doi.org/10.5194/egusphere-2025-2304
Preprint. Discussion started: 17 June 2025

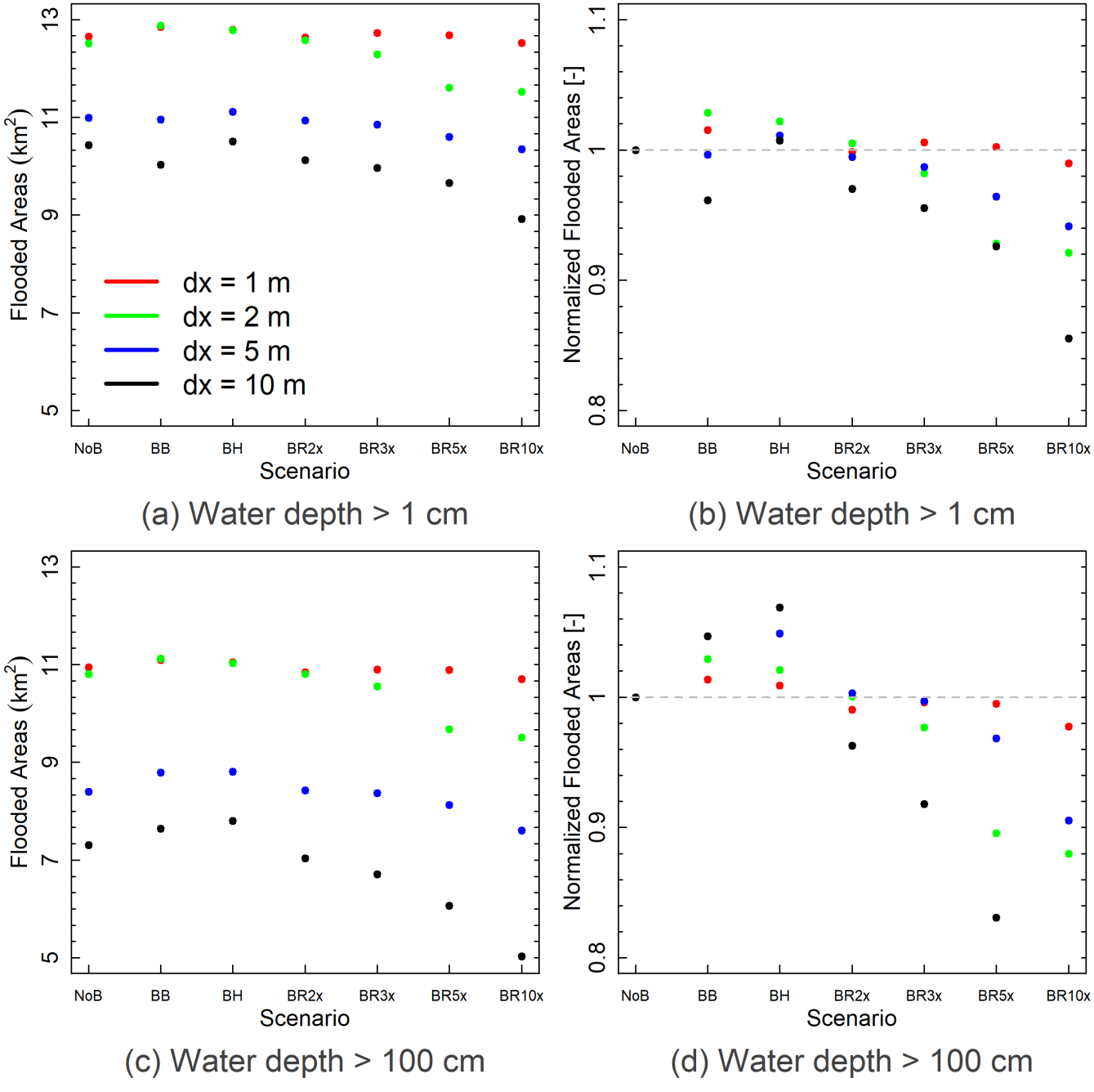

Figure 2. Maximum inundated areas with water depths above (a) 1 and (c) 100 cm for the building scenarios: no building (NoB), buildings blocks (BB), building hole (BH), increased building resistance of 2x (BR2x), 3x (BR3x), 5x BR(5x) and 10x (BR10x) for model resolutions dx = 1, 2, 5 and 10 m. Subfigures (b) and (d) show the normalized maximum inundated areas relative to the corresponding values from the No Building (NoB) scenario.

https://doi.org/10.5194/egusphere-2025-2304
Preprint. Discussion started: 17 June 2025

Although it is seen that the different building representations result in relatively similar flood extents, the differences become noticeable when inspecting the flood maps in detail. Figure 3 presents a close-up of the Ahrweiler region, showing the maximum water depth for various building scenarios: no building (NoB) (top left), building blocks (BB) (top right), building hole (BH) (bottom left) and increased building resistance by 10x (BR10x) (bottom right) for a model resolution of dx = 5 m. In the BB and BH cases, the seen larger flooded areas may be attributed to the same volume of water spreading over a smaller space and going through narrower and more distinct flow paths (i.e. mainly streets), which is the result of the removal or elevation of building footprints. In contrast, the increased roughness resistance leads to a smaller flood extent. This is due to the higher roughness of the building footprint cells, which in term can slow down the spread of the flood, causing the flow to cover a shorter distance. However, based on Figure 2 the differences in flood extents are relatively small. A larger portion of this result has to be attributed to the fact that the simulated floods all cover the whole valley flood from side to side, thus the differences in simulated flood extent is not only influenced by the model setup, but also the geographical situation. Furthermore, as seen in Figure 3, there are also differences in simulated water depths, with the BB and BH scenarios showing greater depths, particularly in comparison to the NoB and increased resistance configurations. This can be attributed to the reduced flow area caused by the exclusion or elevation of buildings in the BH and BB setups, which leads to the concentration of higher water levels in the remaining narrower flow paths. In the NoB and BR scenarios the water volume is also distributed over a larger area, generally leading to lower water depths. Additionally, it should be noted that the flood paths in the NoB and building resistance scenarios are likely more dispersed, as these configurations allow for the redistribution of water over building footprints and involve fewer flow-blocking situations. Since water depths and flooded areas are commonly used as input data for flood impact and risk assessments, our results demonstrate that the representation of buildings in the model can significantly influence the outcomes of these analyses.

https://doi.org/10.5194/egusphere-2025-2304
Preprint. Discussion started: 17 June 2025

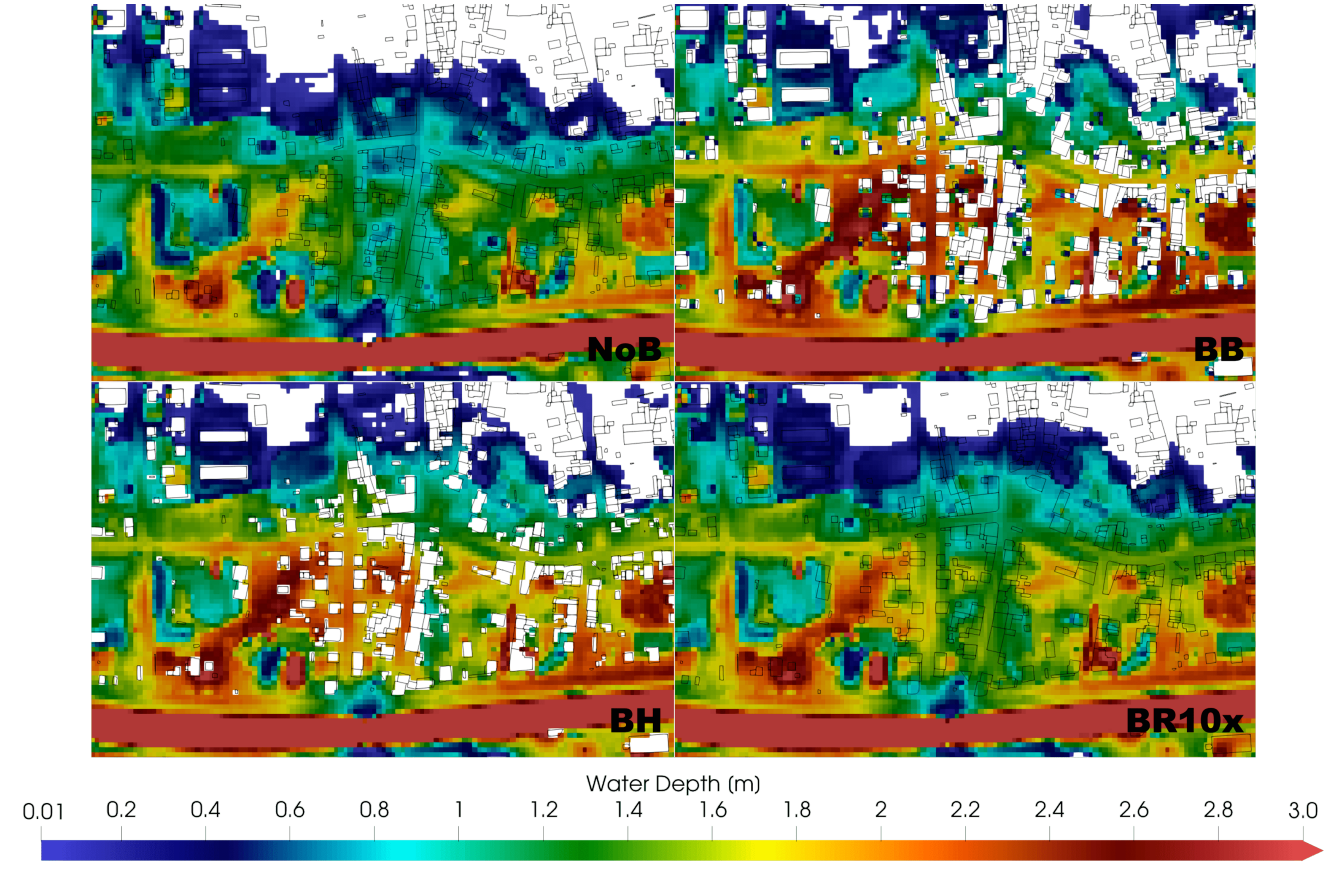

Figure 3. Detailed view at Ahrweiler of the maximum water depth of the building scenarios: no building (NoB) (top left), buildings blocks (BB) (top right), building hole (BH) (bottom left) and increased building resistance of 10x (BR10x) (bottom right) for model resolution dx = 5 m. Black lines represent building footprints based on the LoD1-DE dataset

And it's not just the variations in water depths across different building representations; differences in flow velocities are also observed, as expected from the model setups. Figure 4 provides a detailed view of the maximum water velocity in Ahrweiler for the building scenarios: no building (NoB) (top left), building blocks (BB) (top right), building hole (BH) (bottom left), and increased building resistance by 10x (BR10x) (bottom right), all with a model resolution of dx = 5 m. Significant differences in water velocities are apparent among the four setups. The NoB configuration shows evenly distributed velocities ranging from 2 to 4 m/s, while the BB and BH setups reveal more concentrated, faster flows, with velocities exceeding 4 m/s. The BR10x scenario demonstrates that increasing the roughness Manning value in the building footprint drastically reduces flow velocities, with all cells registering velocities below 2 m/s. Flow velocity is a critical factor in calculating many flood impact indicators, such as human instability or floating car maps (Apel et al., 2022; Khosh Bin Ghomash et al., 2025a). Our findings clearly indicate that the choice of building representation can substantially influence simulated urban flood water flows, ultimately affecting the outcomes of flood impact and risk assessments.

https://doi.org/10.5194/egusphere-2025-2304
Preprint. Discussion started: 17 June 2025

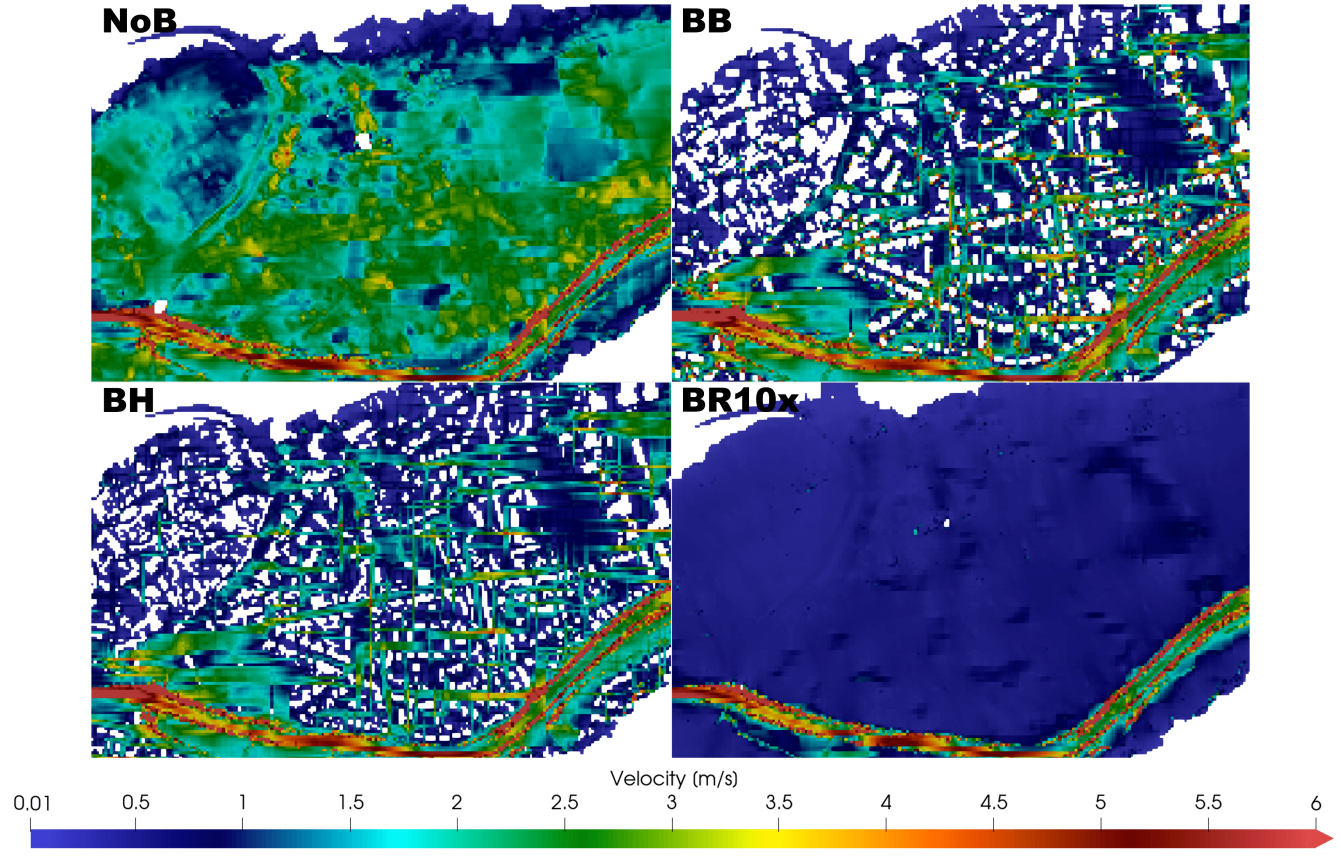

Figure 4. Detailed view at Ahrweiler of the maximum water velocity of the building scenarios: no building (NoB) (top left), buildings blocks (BB) (top right), building hole (BH) (bottom left) and increased building resistance of 10x (BR10x) (bottom right) for model resolution dx = 5 m.

To gain a more quantitative understanding of how different building representations influence water depth and velocity, Figure 5 shows the distributions of maximum flow depths (for cells exceeding 0.01 m) and maximum flow velocities (for velocities above 0.01 m/s) across the whole simulation domain. The comparison includes four building representation scenarios: no buildings (NoB), building blocks (BB), building holes (BH), and increased building resistance by a factor of 10 (BR10x), all at a resolution of dx = 5 m. Regarding water depth, the BB and BH scenarios exhibit a greater number of cells with higher water depths, aligning with the trends observed in Figure 3. In contrast, the BR10x scenario yields the lowest water depths, which is also consistent with Figure 3. As for flow velocity, the increased resistance approach (BR10x) leads to more extensive flooded areas characterized by very low velocities, mostly below 1 m/s. Conversely, the BB and BH representations show larger areas experiencing significantly higher velocities, indicating more dynamic and realistic flow behavior. These results reinforce the view that the BB and BH approaches better capture the flow dynamics compared to the increased resistance method. Overall,

https://doi.org/10.5194/egusphere-2025-2304
Preprint. Discussion started: 17 June 2025

these findings support the conclusion drawn by Néelz and Pender (2007), which suggested that while increased resistance may be adequate for simulating flood extents, it is likely to produce inaccurate representations of urban flood dynamics.

https://doi.org/10.5194/egusphere-2025-2304
Preprint. Discussion started: 17 June 2025

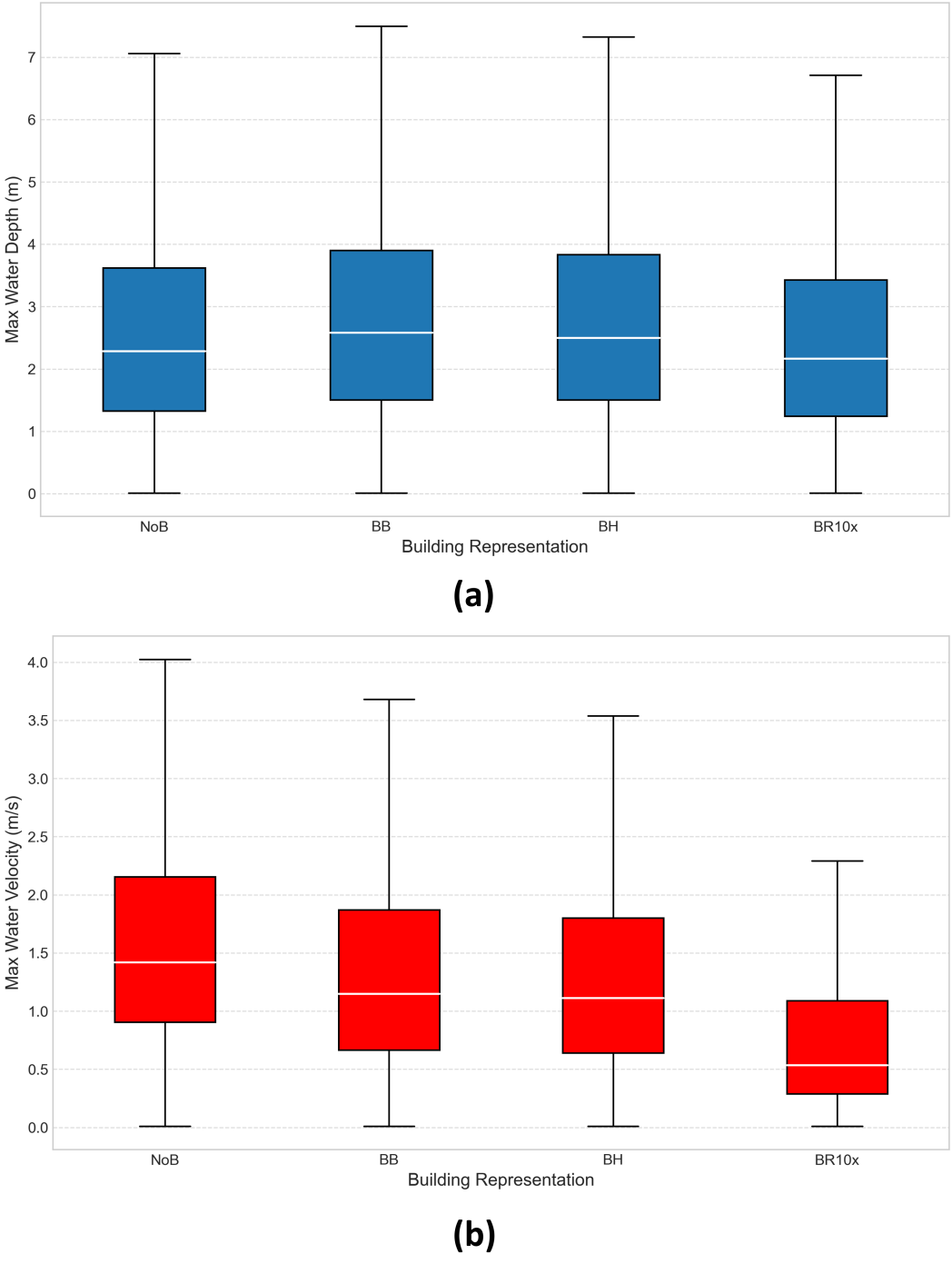

Figure 5. Distributions of (a) maximum flow depths (cells above 0.01 m) and (b) maximum flow velocities (velocities above 0.01 m/s) in the simulation domain for building scenarios: no building (NoB), buildings blocks (BB), building hole (BH), and increased building resistance of 10x (BR10x). The results are for the dx = 5 m setups.

https://doi.org/10.5194/egusphere-2025-2304
Preprint. Discussion started: 17 June 2025

4.2 Flood impact

As seen in the previous sections, although different building representations lead to relatively similar flood extents, substantial differences emerge in the simulated flow dynamics, particularly in velocity and depth patterns. These dynamic variations have important implications for flood impact assessments that go beyond mere inundation mapping. To demonstrate this, we calculated human instability maps for each building representation using the method proposed by Jonkman and Penning-Rowsell (2008), which evaluates the potential for people to lose stability in floodwaters based on combined water depth and velocity. We adopted a conservative critical threshold of 1 m^2/s, which reflects the instability risk for lightweight individuals and serves as a buffer for uncertainties inherent in hydrodynamic modeling, especially regarding velocity estimates near structures and sharp gradients.

The resulting instability areas differ notably among the scenarios. For the NoB, BH, and BR10x configurations, the spatial extents where human instability is likely were computed as 9.81, 9.03, and 6.4 km^2, respectively, for simulations conducted at a 5 m resolution. These values underscore how different representations of buildings in the model can significantly influence hazard estimates that are critical to public safety. For illustrative purposes, Figure 6 displays a detailed view of the human instability indicator in a subsection of Ahrweiler. The maps for the NoB (top), BH (middle), and BR10x (bottom) scenarios visibly contrast the resulting risk zones. The BR10x scenario, which incorporates higher building resistance, shows a markedly reduced area of human instability, indicating that increased structural resistance alters local flow paths and attenuates velocities that would otherwise pose a hazard to human life.

These findings highlight a crucial point: while flood extent alone may suggest minimal sensitivity to building representation, the underlying hydrodynamic behavior—and by extension, human exposure and risk—can vary substantially. This has direct implications for flood risk management, emergency planning, and urban resilience strategies. If flow velocities and resulting human instability zones are underestimated or overestimated due to simplified or inappropriate building representations, mitigation measures may be misallocated, and evacuation planning may fail to protect vulnerable populations adequately. Thus, careful consideration of building representation in urban flood modeling is essential not only for hydraulic realism but also for informing high-stakes decisions in disaster preparedness and response.

Lastly, since computational time is a key factor in selecting data for hydrodynamic models, it's important to highlight that the different building representations lead to only minor variations in computational cost. With the simulation runtimes on a single Nvidia A100 GPU being approximately in the range of 5, 28, 321, and 1554 minutes for grid resolutions of 10, 5, 2, and 1 meter, respectively. Naturally, these times can be significantly reduced by increasing the number of GPUs used in the simulations.

https://doi.org/10.5194/egusphere-2025-2304
Preprint. Discussion started: 17 June 2025

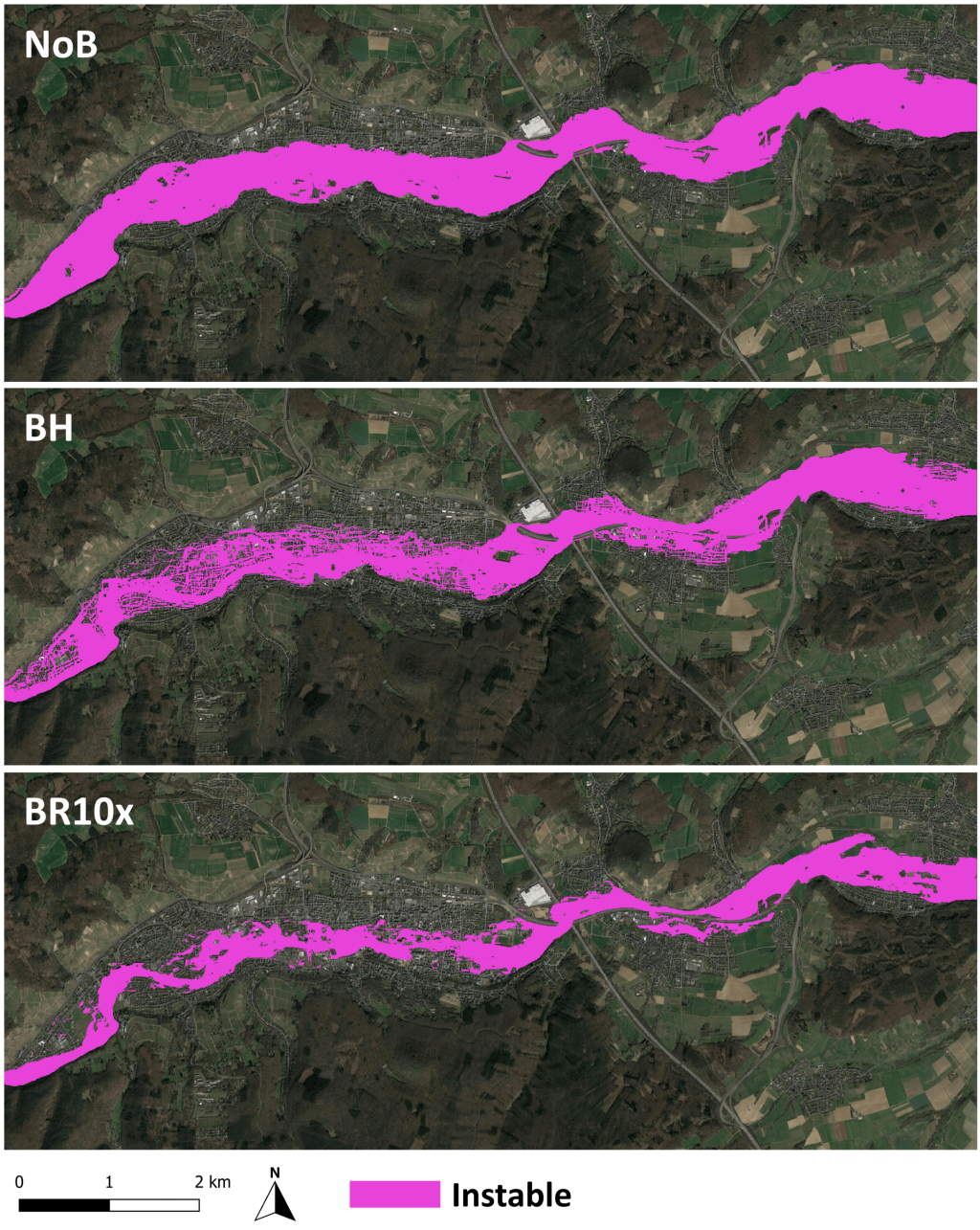

Figure 6. Detailed view at Ahrweiler of the human instability indicator for the building scenarios: no building (NoB) (left), building hole (BH) (center) and increased building resistance of 10x (BR10x) (right) for model resolution dx = 5 m. The critical value for human instability was set to 1 $m^2 s^{-1}$, following Jonkman and Penning-Rowsell (2008). Satellite imagery: © Google Earth 2025.

https://doi.org/10.5194/egusphere-2025-2304
Preprint. Discussion started: 17 June 2025

4.3 Comparison to observations

Here, we compare the simulation results to observations from the actual 2021 flood event. This includes the observed flood extent provided by the State Agency for the Environment of Rhineland-Palatinate (LfU – Landesamt für Umwelt), as well as water depth measurements reported by residents at 65 locations (Apel et al., 2022).

In order to compare the resulting simulated flood extents to the observed flood extent of the 2021 flood event, a set of metrics are employed. These metrics are computed by evaluating the maximum inundation maps of the RIM2D simulations against the observed flood extent. Initially, cells are categorized based on Table 2. For this classification, RIM2D results are termed "simulated" and the 2021 observed extent "observed". A confusion map is generated from each comparison, providing the total counts for the indices presented in Table 2. These counts are then utilized to compute the domain-wide inundation metrics as illustrated in Table 3. These metrics are based on works by Wing et al. (2017) and Bernini and Franchini (2013).

		Simulated	
		Wet	Dry
Observed	Wet	True Positive (TP)	False Negative (FN)
	Dry	False Positive (FP)	True Negative (TN)

Table 2. Inundation confusion matrix. Each cell in the domain for a given simulation is compared to the corresponding cell in the observed grid and classified according to this table.

Metric	Equation	Poor	Perfect	Description
Critical Success Index	$\frac{TP}{TP+FP+FN}$	0	1	ratio of accurate wet cells to total wet cells and missed wet cells
Hit Rate	$\frac{TP}{TP+FN}$	0	1	portion of observed wet cells reproduced by the model
Bias Percentage Indicator	$100\left(\frac{TP+FP}{TP+FN}-1\right)$	-100 or 100	0	relative percentage error of the final extent of the flooded area

Table 3. Flood inundation performance metrics

Figure 7 shows the comparison of flooded areas using the Critical Success Index (CSI), Hit Rate (HR), and Bias Percentage Indicator (BI). The indices are presented for various building scenarios: no building (NoB), buildings blocks (BB), building hole (BH), and increased building resistance by factors of 2x (BR2x), 3x (BR3x), 5x (BR5x), and 10x (BR10x), across model resolutions of dx = 1, 2, 5, and 10 m. Overall, the RIM2D model demonstrates high accuracy in reproducing flood extents across all building scenarios, with all scenarios achieving high scores on all three indices. Even the scenario without buildings in the model (NoB) attains high scores (e.g., CSI scores above 0.80 in Figure 7a). These results are in line with findings of Khosh Bin Ghomash et al. (2025b) that showed that calibration is not really necessary for simulation of flood extents in Ahr valley at a good accuracy but is more needed for simulation of flow dynamics in the river channel. This finding, however, has to be partly attributed to the widespread flooding of the valley from from side to side. More differentiation between the different

https://doi.org/10.5194/egusphere-2025-2304
Preprint. Discussion started: 17 June 2025

model setups has to be expected in situations with less confined floodplains. In general from the figure it is seen typically higher resolutions across all setups result in higher scores compared to lower resolutions, which is an expected result. It is worth noting that the differences in performance scores between the various building representation scenarios are more pronounced in the coarser resolution setup (dx = 10 m) compared to the finer resolution configurations. This may be attributed to the larger cell size in the coarser grid, which causes building footprints to occupy a greater spatial extent and thus exert a stronger influence on flow dynamics. This observation highlights the critical importance of accurate building representation in coarser-resolution models, which are often favored due to their lower computational demands or the unavailability of high-resolution data.

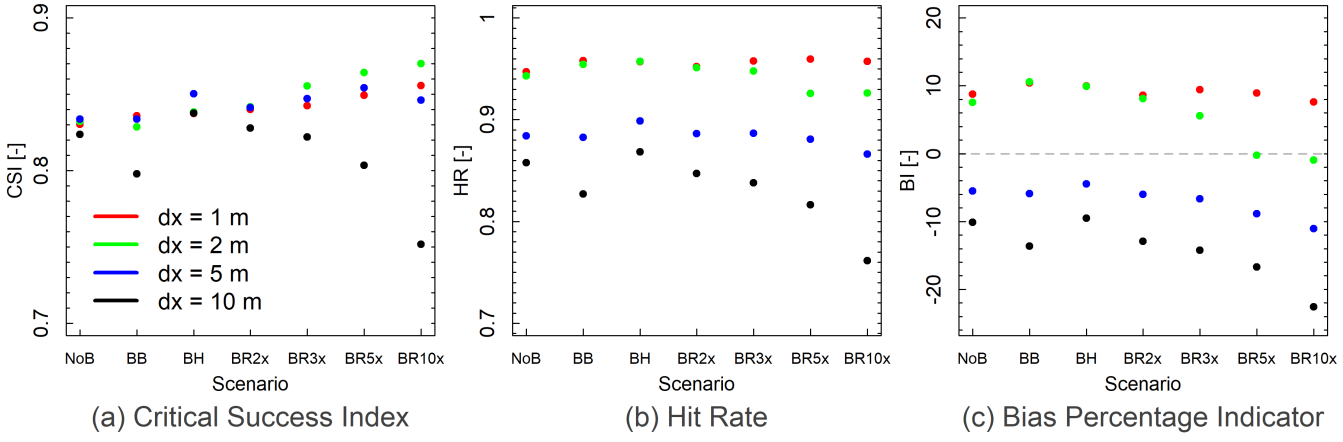

Figure 7. Comparison of flooded areas with the indices' Critical Success Index (CSI), Hit Rate (HR) and Bias Percentage Indicator (BI). The flooded areas of the building scenarios: no building (NoB), buildings blocks (BB), building hole (BH), increased building resistance of 2x (BR2x), 3x (BR3x), 5x BR(5x) and 10x (BR10x) for model resolutions dx = 1, 2, 5 and 10 m are presented.

In order to quantify the performance in terms of flood depths, simulated water depths in the domain are compared with observation water marks reported by the residents. In this context it has to be noted that the observations were not systematically surveyed, but simply reported by the residence without knowledge on how the measurements were taken or what the vertical datum for the measurements were. Thus there is an unknown quantity of uncertainty associated to the observations, which needs to be taken into account when interpreting the performance values. For the quantification of the performance two indicators, Bias and Root Mean Square Error (RMSE), were used. The Bias is calculated as follows:

$$\text{Bias} = \frac{1}{n}\sum_{i=1}^{n}(\hat{y}_i - y_i)$$

and RMSE is calculated as:

$$\text{RMSE} = \sqrt{\frac{1}{n}\sum_{i=1}^{n}(\hat{y}_i - y_i)^2}$$

In both equations:

- n is the total number of observations.
- $\hat{y}_i$ represents the simulated values.

https://doi.org/10.5194/egusphere-2025-2304
Preprint. Discussion started: 17 June 2025

– y_i represents the observed values.

Figure 8 presents the resulting RMSE and Bias values for all the building representation methods for resolutions 1, 2, 5 and 10 m. The evaluation of model performance across different building representation scenarios and grid resolutions reveals mainly mixed insights. At finer resolutions (dx = 1 m and 2 m), resistance-based approaches yield lower RMSE values compared to explicit building representations (BB and BH); however, at coarser resolutions (dx = 5 and 10 m), the BB and BH setups result in lower RMSE values. With regards to bias, resistance-based scenarios exhibit increasingly negative bias, indicating a systematic underestimation of water depths. In contrast, at coarser resolutions, the BB and BH scenarios maintain a more balanced bias—closer to zero, where they also tend to outperform other methods in terms of RMSE. Generally, BB and BH offer a more physically realistic representation of urban structures and demonstrate acceptable performance across varying resolutions, especially in coarser grids where building representation exerts a stronger influence on flow dynamics. Most importantly, these results show uncalibrated model results. For getting more accurate simulations of water depths calibration is essential (Khosh Bin Ghomash et al., 2025b), because in essence the roughness calibration has to compensate the effects of resolution on flood dynamics and thus flood depths. Calibration may thus very likely shift the relative performance of different building representation approaches. Nonetheless, the results clearly highlight that the choice of building representation leads to notable differences in simulated water depths, underlining its importance in urban flood modeling. Therefore, selecting an appropriate building representation should consider calibration potential and the intended application of the model.

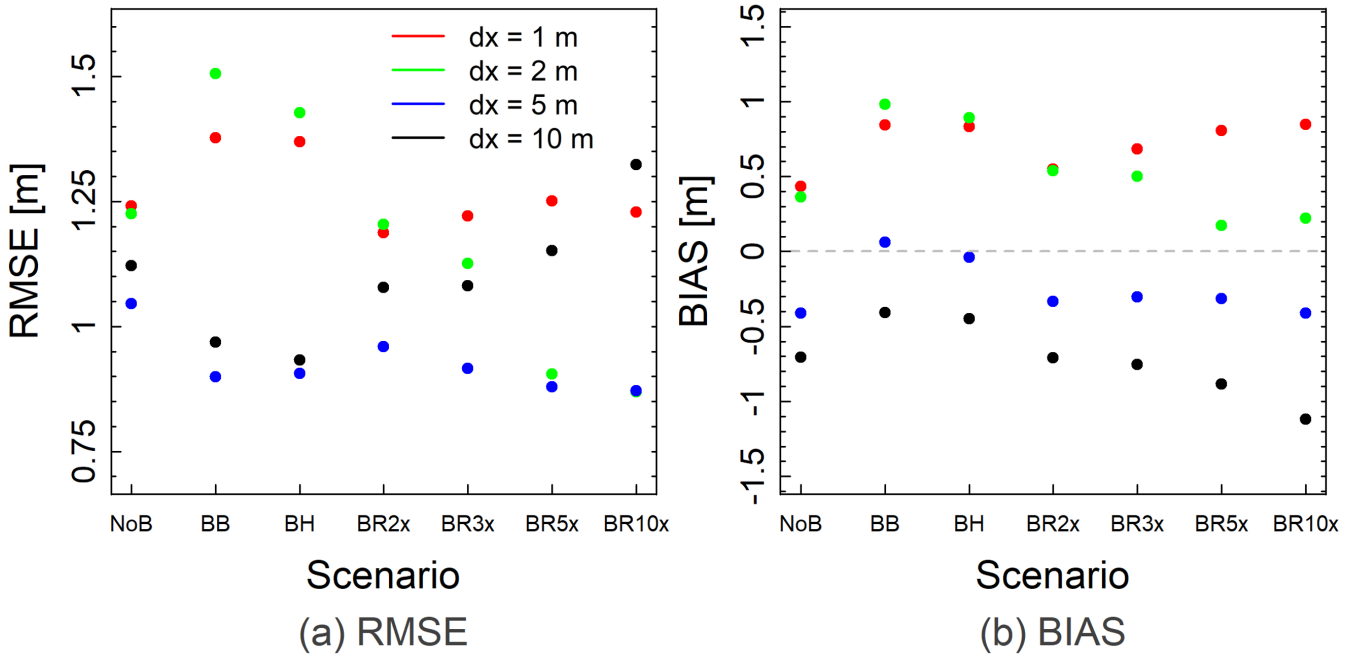

Figure 8. Calculated RMSE (a) and Bias (b) for comparison of simulated water depths to observed in 65 locations in the domain for the building scenarios: no building (NoB), buildings blocks (BB), building hole (BH), increased building resistance of 2x (BR2x), 3x (BR3x), 5x BR(5x) and 10x (BR10x) for model resolutions dx = 1, 2, 5 and 10 m.

https://doi.org/10.5194/egusphere-2025-2304
Preprint. Discussion started: 17 June 2025

5 Conclusions

This study assessed the influence of different building representation techniques on flood hydrodynamic modeling outcomes, using the 2021 Ahr Valley flood as a test case. By evaluating three building representation methods — Building Block (BB), Building Hole (BH), and Building Resistance (BR) — across various model resolutions, we demonstrated that the choice of building representation plays a significant role particularly for the simulation of water depths and flow velocities.

Our findings indicate that while all building representation scenarios generally produced reasonable flood extents-with differences of up to 15%- there were more pronounced discrepancies in the finer details of water depth and velocity distributions. The BB and BH methods consistently resulted in greater food extents, water depths and higher velocities, especially in urban areas where buildings obstructed or redirected floodwaters. The increased resistance setups on the other hand resulted in smaller extents with slower and shallower flow. These variations can have profound implications for flood impact assessments, as deeper and faster-flowing water can lead to more severe flood impacts, such as heightened risks of human instability, infrastructure damage, and increased flood hazard zones.

Furthermore, the study revealed a strong interaction between model resolution and building representation accuracy. It was demonstrated that the influence of building representation on simulated flood extent is more pronounced at coarser spatial resolutions, which are often favored due to reduced computational demands or limited availability of high-resolution data. At these coarser resolutions, variations in building representation led to larger discrepancies in the simulated flood extents. Moreover with regards to accuracy, at coarser resolutions (e.g., dx = 10 m), the BH and BB methods emerged as the most reliable approach, producing the most accurate flood extent predictions when compared to observed flood data. This is likely due to the methods ability to account for the physical blocking effect of buildings, even when individual structures are less precisely defined at coarser scales. In contrast, at finer resolutions (e.g., dx = 1-2 m), the increased resistance method provided slightly better flood extent predictions in the presented case study. This comes, however, at the cost of large deviations of the simulated water depths and velocities. The increased resistance method was shown to highly underestimate the flow depth and velocity during the simulations compared to the other building representation methods. This underscores the potential risks of oversimplifying building representation in flood modeling. Simplified approaches, such as using a uniform resistance factor, may lead to underestimations of flood impacts, particularly in densely built-up areas. Given that water depths and velocities directly inform flood risk assessments and potentially also flood forecasts and disaster management, such inaccuracies could lead to significant errors in evaluating potential flood damage, human safety, and emergency response planning. Moreover, it should be pointed out that for optimized flow depth and velocity predictions, calibration would be required, regardless of the building representation method used.

In practical terms, this research provides important guidance for flood risk practitioners and modelers, especially for modeling endeavors in the studied area. If flood extent is the only concern, then a coarse resolution model with any of the building representation techniques, even the increased resistance approach might be an appropriate choice. However, as the flood extent in this case study is confined by a narrow valley floor floodplain, the latter finding cannot be generalized. Moreover, for all other applications, where the flood dynamics are important, the BH or BB approaches should be used. The resolution to be

https://doi.org/10.5194/egusphere-2025-2304
Preprint. Discussion started: 17 June 2025

chosen depends on the actual problem at hand, but from the presented results, the 5 m resolution appears to be sufficient to represent the urban flood dynamics in typical Central European settings-a finding also in line with other recent flood modeling studies conducted in similar regions (Apel et al., 2024; Khosh Bin Ghomash et al., 2025a).

In conclusion, the presented study and literature highlight the importance of the representation of buildings urban flood modeling, affecting the accuracy and reliability of flood extent and flow dynamics simulation as well as impact assessments. Although this is shown for a single case study only, the supporting literature and the underlying theoretical considerations support a generalization of this finding beyond the test study.

For even more realistic urban flow simulations, future studies should consider more complex building representations that account for factors such as flow-through effects, which could further refine flood modeling accuracy in complex urban landscapes. Additionally, expanding this research to different flood events, urban configurations, and building structures will help establishing a larger empirical database for generalized guidelines for selecting appropriate building representation methods. By incorporating these considerations, hydrodynamic models can better inform flood risk management, adaptation planning, and mitigation strategies, ultimately contributing to more resilient urban communities in the face of increasing flood hazards driven by climate change and urbanization.

Code availability. RIM2D is available at https://git.gfz-potsdam.de/hydro/rfm/rim2d (last access: 16 April 2025). RIM2D is open-source for scientific use under the EUPL1.2 license. Access is granted upon request. The simulations were performed with version 0.2.

Data availability. The land cover raster, which was used to assign roughness values to the simulation domain, is openly accessible at https://www.mundialis.de/en/germany-2020-land-cover-based-on-sentinel-2-data/ (last access: 16 April 2025).

The 1m DTM has recently been made available at https://gdz.bkg.bund.de/index.php/default/digitale-geodaten/digitale-gelandemodelle/digitales-oberfaechenmodell-dom1.html (last access: 16 April 2025).

Flood extent data were obtained from the UFZ data investigation portal via https://doi.org/10.48758/ufz.14607 (Najafi et al., 2024).

The LoD1-DE building dataset can be requested and attained from the German Federal Agency for Cartography and Geodesy (BKG) via https://gdz.bkg.bund.de/index.php/default/3d-gebaudemodelle-lod1-deutschland-lod1-de.html (last access: 16 April 2025).

Acknowledgements. This research was performed within the frame of the DIRECTED project (https://directedproject.eu/). Funding of the DIRECTED project within the European Union's Horizon Europe – the Framework Programme for Research and Innovation (grant agreement No. 101073978, HORIZON-CL3-2021-DRS-01) is gratefully acknowledged. This work utilized high-performance computing resources made possible by funding from the Ministry of Science, Research and Culture of the State of Brandenburg (MWFK) and are operated by the IT Services and Operations unit of the Helmholtz Centre Potsdam.

https://doi.org/10.5194/egusphere-2025-2304
Preprint. Discussion started: 17 June 2025

Author contributions. SKBG: Conceptualization, Methodology, Investigation, Simulation, Software, Analysis, Visualization, Writing; NDN: Conceptualization, Investigation; HA: Software, Conceptualization, Writing, Review

Competing interests. The authors declare no conflicts of interests.

Appendix A: Supplementary Material: reconstructed water level timeseries at the Altenahr gauge

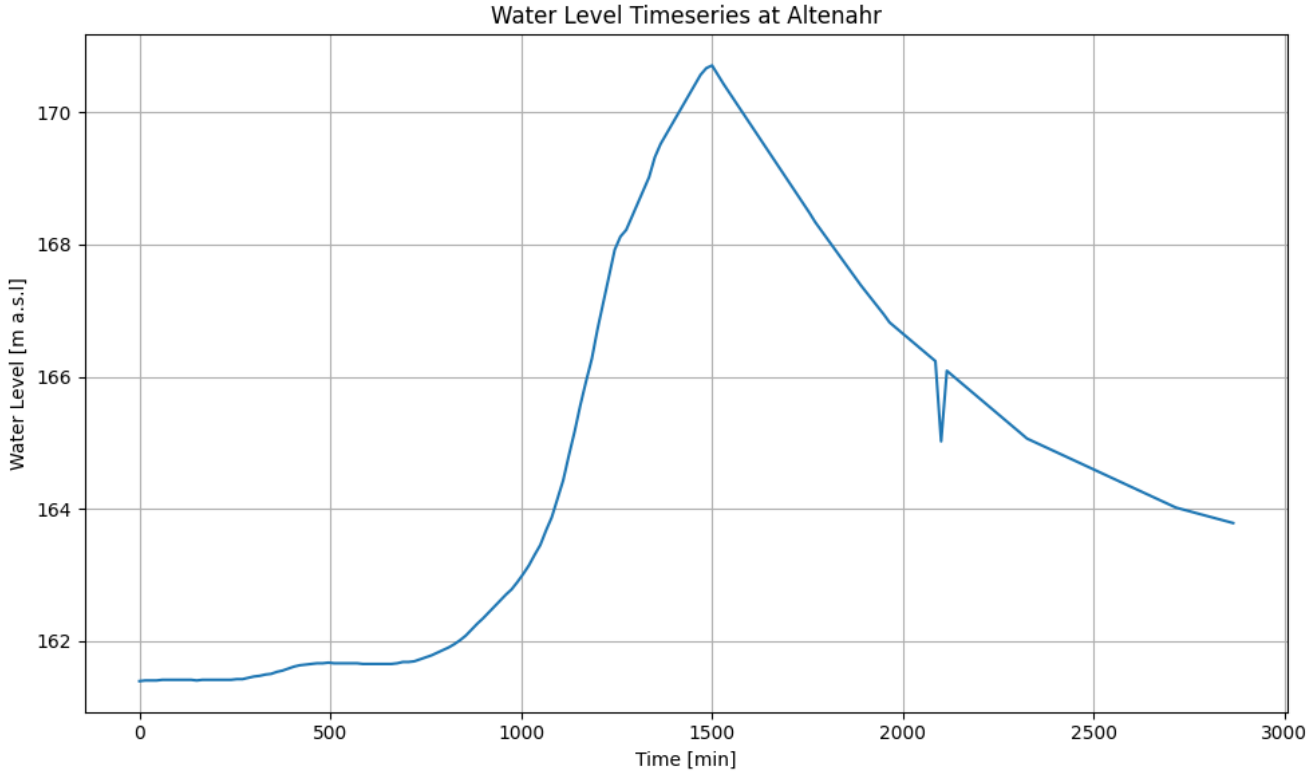

Figure A1. The reconstructed water level timeseries at the Altenahr gauge, used as boundary condition in the model. The first timestep in the timeseries is at 2021-7-14 12:30:00.

https://doi.org/10.5194/egusphere-2025-2304
Preprint. Discussion started: 17 June 2025

References

Alcrudo, F.: Mathematical modelling techniques for flood propagation in urban areas, Project report: IMPACT Project, 2004.

Alipour, A., Jafarzadegan, K., and Moradkhani, H.: Global sensitivity analysis in hydrodynamic modeling and flood inundation mapping, Environmental Modelling & Software, 152, 105 398, 2022.

Apel, H., Vorogushyn, S., and Merz, B.: Brief communication: Impact forecasting could substantially improve the emergency management of deadly floods: case study July 2021 floods in Germany, Natural Hazards and Earth System Sciences, 22, 3005–3014, https://doi.org/10.5194/nhess-22-3005-2022, 2022.

Apel, H., Benisch, J., Helm, B., Vorogushyn, S., and Merz, B.: Fast urban inundation simulation with RIM2D for flood risk assessment and forecasting, Frontiers in Water, 6, 1310 182, 2024.

Bates, P. D., Horritt, M. S., and Fewtrell, T. J.: A simple inertial formulation of the shallow water equations for efficient two-dimensional flood inundation modelling, Journal of Hydrology, 387, 33–45, https://doi.org/10.1016/j.jhydrol.2010.03.027, 2010.

Bernini, A. and Franchini, M.: A rapid model for delimiting flooded areas, Water resources management, 27, 3825–3846, 2013.

Bruwier, M., Mustafa, A., Aliaga, D. G., Archambeau, P., Erpicum, S., Nishida, G., Zhang, X., Pirotton, M., Teller, J., and Dewals, B.: Influence of urban pattern on inundation flow in floodplains of lowland rivers, Science of the Total Environment, 622, 446–458, 2018.

Caviedes-Voullième, D., Fernández-Pato, J., and Hinz, C.: Performance assessment of 2D Zero-Inertia and Shallow Water models for simulating rainfall-runoff processes, Journal of hydrology, 584, 124 663, 2020.

De Almeida, G. A. and Bates, P.: Applicability of the local inertial approximation of the shallow water equations to flood modeling, Water Resources Research, 49, 4833–4844, 2013.

de Almeida, G. A., Bates, P., Freer, J. E., and Souvignet, M.: Improving the stability of a simple formulation of the shallow water equations for 2-D flood modeling, Water Resources Research, 48, 2012.

Dewals, B., Bruwier, M., Pirotton, M., Erpicum, S., and Archambeau, P.: Porosity models for large-scale urban flood modelling: A review, Water, 13, 960, 2021.

Falter, D., Dung, N., Vorogushyn, S., Schröter, K., Hundecha, Y., Kreibich, H., Apel, H., Theisselmann, F., and Merz, B.: Continuous, large-scale simulation model for flood risk assessments: proof-of-concept, Journal of Flood Risk Management, 9, 3–21, https://doi.org/10.1111/jfr3.12105, 2014.

Hunter, N. M., Bates, P., Neelz, S., Pender, G., Villanueva, I., Wright, N., Liang, D., Falconer, R. A., Lin, B., Waller, S., et al.: Benchmarking 2D hydraulic models for urban flooding, in: Proceedings of the institution of civil engineers-water management, vol. 161, pp. 13–30, Thomas Telford Ltd, 2008.

Iliadis, C., Glenis, V., and Kilsby, C.: Representing buildings and urban features in hydrodynamic flood models, Journal of Flood Risk Management, 17, e12 950, 2024.

Jiang, W., Yu, J., Wang, Q., and Yue, Q.: Understanding the effects of digital elevation model resolution and building treatment for urban flood modelling, Journal of Hydrology: Regional Studies, 42, 101 122, 2022.

Jonkman, S. and Penning-Rowsell, E.: Human instability in flood flows 1, JAWRA Journal of the American Water Resources Association, 44, 1208–1218, 2008.

Khosh Bin Ghomash, S., Caviedes-Voullieme, D., and Hinz, C.: Effects of erosion-induced changes to topography on runoff dynamics, Journal of Hydrology, 573, 811–828, 2019.

https://doi.org/10.5194/egusphere-2025-2304
Preprint. Discussion started: 17 June 2025

Khosh Bin Ghomash, S., Bachmann, D., Caviedes-Voullième, D., and Hinz, C.: Impact of rainfall movement on flash flood response: A synthetic study of a semi-arid mountainous catchment, Water, 14, 1844, 2022.

Khosh Bin Ghomash, S., Bachmann, D., Caviedes-Voullième, D., and Hinz, C.: Effects of Within-Storm Variability on Allochthonous Flash Flooding: A Synthetic Study, Water, 15, 645, 2023.

Khosh Bin Ghomash, S., Apel, H., and Caviedes-Voullième, D.: Are 2D shallow-water solvers fast enough for early flood warning? A comparative assessment on the 2021 Ahr valley flood event, Natural Hazards and Earth System Sciences, 24, 2857–2874, 2024.

Khosh Bin Ghomash, S., Apel, H., Schröter, K., and Steinhausen, M.: Rapid high-resolution impact-based flood early warning is possible with RIM2D: a showcase for the 2023 pluvial flood in Braunschweig, Natural Hazards and Earth System Sciences, 25, 1737–1749, https://doi.org/10.5194/nhess-25-1737-2025, 2025a.

Khosh Bin Ghomash, S., Yeste, P., Apel, H., and Nguyen, V. D.: Monte Carlo-based sensitivity analysis of the RIM2D hydrodynamic model for the 2021 flood event in western Germany, Natural Hazards and Earth System Sciences, 25, 975–990, 2025b.

Kim, B., Sanders, B. F., Famiglietti, J. S., and Guinot, V.: Urban flood modeling with porous shallow-water equations: A case study of model errors in the presence of anisotropic porosity, Journal of Hydrology, 523, 680–692, 2015.

Merz, B., Kuhlicke, C., Kunz, M., Pittore, M., Babeyko, A., Bresch, D. N., Domeisen, D. I., Feser, F., Koszalka, I., Kreibich, H., et al.: Impact forecasting to support emergency management of natural hazards, Reviews of Geophysics, 58, e2020RG000 704, 2020.

Mohr, S., Ehret, U., Kunz, M., Ludwig, P., Caldas-Alvarez, A., Daniell, J. E., Ehmele, F., Feldmann, H., Franca, M. J., Gattke, C., et al.: A multi-disciplinary analysis of the exceptional flood event of July 2021 in central Europe. Part 1: Event description and analysis, Natural Hazards and Earth System Sciences Discussions, 2022, 1–44, 2022.

Najafi, H., Shrestha, P., Rakovec, O., Thober, S., Kumar, R., and Samaniego-Eguiguren, L.: Data and Scripts for Advancing a High-Resolution Impact-based Early Warning System for Riverine Flooding, Helmholtz-Centre for Environmental Research [code and data set], 2024.

Neal, J., Schumann, G., Fewtrell, T., Budimir, M., Bates, P., and Mason, D.: Evaluating a new LISFLOOD-FP formulation with data from the summer 2007 floods in Tewkesbury, UK, Journal of Flood Risk Management, 4, 88–95, https://doi.org/10.1111/j.1753-318x.2011.01093.x, 2011.

Néelz, S. and Pender, G.: Sub-grid scale parameterisation of 2D hydrodynamic models of inundation in the urban area, Acta Geophysica, 55, 65–72, 2007.

Nithila Devi, N. and Kuiry, S. N.: A novel local-inertial formulation representing subgrid scale topographic effects for urban flood simulation, Water Resources Research, 60, e2023WR035 334, 2024.

Riembauer, G., Weinmann, A., Xu, S., Eichfuss, S., Eberz, C., and Neteler, M.: Germany-wide Sentinel-2 based land cover classification and change detection for settlement and infrastructure monitoring, in: Proceedings of the 2021 Conference on Big Data from Space, Virtual, pp. 18–20, 2021.

Schäfer, A., Mühr, B., Daniell, J., Ehret, U., Ehmele, F., Küpfer, K., Brand, J., Wisotzky, C., Skapski, J., Rentz, L., et al.: Hochwasser Mitteleuropa, Juli 2021 (Deutschland), CEDIM Forensic Disaster Analysis Group Bericht, 2021.

Schubert, J. E. and Sanders, B. F.: Building treatments for urban flood inundation models and implications for predictive skill and modeling efficiency, Advances in Water Resources, 41, 49–64, 2012.

Sharma, V. C. and Regonda, S. K.: Two-dimensional flood inundation modeling in the Godavari River Basin, India—Insights on model output uncertainty, Water, 13, 191, 2021.

Shen, J. and Tan, F.: Effects of DEM resolution and resampling technique on building treatment for urban inundation modeling: a case study for the 2016 flooding of the HUST campus in Wuhan, Natural Hazards, 104, 927–957, 2020.

https://doi.org/10.5194/egusphere-2025-2304
Preprint. Discussion started: 17 June 2025

Skougaard Kaspersen, P., Høegh Ravn, N., Arnbjerg-Nielsen, K., Madsen, H., and Drews, M.: Comparison of the impacts of urban development and climate change on exposing European cities to pluvial flooding, Hydrology and Earth System Sciences, 21, 4131–4147, 2017.

Truedinger, A. J., Jamshed, A., Sauter, H., and Birkmann, J.: Adaptation after Extreme Flooding Events: Moving or Staying? The Case of the Ahr Valley in Germany, Sustainability, 15, 1407, 2023.

Wang, X., Cao, Z., Pender, G., and Neelz, S.: Numerical modelling of flood flows over irregular topography, in: Proceedings of the Institution of Civil Engineers-Water Management, vol. 163, pp. 255–265, Thomas Telford Ltd, 2010.

Wing, O. E., Bates, P. D., Sampson, C. C., Smith, A. M., Johnson, K. A., and Erickson, T. A.: Validation of a 30 m resolution flood hazard model of the conterminous United States, Water Resources Research, 53, 7968–7986, 2017.